Vibro-acoustical Modal Analysis : Reciprocity, Model Symmetry and Model Validity

Katrien Wyckaert
LMS International
Interleuvenlaan 68
3001 Leuven
Belgium

Fülöp Augusztinovicz
Mechanical Engineering Department, Division PMA
Katholieke Universiteit Leuven
3001 Leuven
Belgium

ABSTRACT

Coupling between the structural dynamical behaviour of a system and its interior acoustical characteristics, is an important phenomenon in many applications. For low frequency applications, a modal approach can be very useful to describe this vibro-acoustical coupling. Based upon combined vibrational/acoustical FRF measurements, either with respect to acoustical or to structural excitation, modal vibro-acoustical analysis can be carried out.

This paper presents a consolidation of the theory behind the vibro-acoustical modal model. The model formulation is shown to be a non-symmetrical formulation. It is shown that this is not contradictory to the well known vibro-acoustical reciprocity principle. The implications of this non-symmetry for the modal model are discussed. It is pointed out which variables must be measured, that allow a consistent model formulation.

The theory is illustrated by measurements on an experimental vibro-acoustical system, consisting of a rigid cavity, with one flexible wall. Experimental constraints and requirements and analysis results are discussed.

1. INTRODUCTION

When considering the global vibro-acoustical problem of enclosures, coupling exists between the acoustical response in the cavity and structural excitation, whereas also the structural response is coupled to acoustical excitation sources in the cavity.

Vibro-acoustical coupling implies that the acoustical and vibratory system behaviour are not independent from each other. The global system behaviour has to be considered as one unity.

In order to fully understand and model the vibro-acoustical problem, vibro-acoustical modal analysis can be considered, which aims at identifying an (interdependent) model both for the vibratory and the acoustical behaviour of a system.

Modal analysis is an appropriate tool to solve this problem in the lower frequency area. However, the correct physical quantities must be measured. Also it is important to understand how these quantities relate to each other, and which model formulation is consistent. A special focus must be put on vibro-acoustical reciprocity, implying a special form of non-symmetry in the consistent model formulation. This has repercussions on the choice of the excitation method, which can be either acoustical or structural.

2. MODEL FORMULATION

notation :

	p	pressure (N/m^2)
	$\ddot{x}$	acceleration (m/s^2)
	q	volume velocity (m^3/s)
	f	structural (point) force (N)
	ρ	fluid density (kg/m^3)
	c	speed of sound in fluid (m/s)

In order to understand the equations describing the vibro-acoustical behaviour of coupled systems, one can start from the finite element formulations (see reference [1]). The (finite element) equation of motion for the structural vibrational behaviour under external structural loading conditions, as well as under coupled acoustical loading, looks as follows:

$$[-\omega^2 M^s - i\omega C^s + K^s]\{x\} = \{f\} + \{l_p\} \tag{1}$$

with

M^S, C^s, K^s	the structural mass, damping and stiffness matrices	
$\{f\}$	the externally applied forces	
$\{l_p\} = \int_{s_b} p\,dS$	the acoustical pressure loading vectors over the boundary surfaces s_b of the cavity	(2)

On the other hand, when considering the acoustical problem, the acoustical pressure response in the cavity is caused by acoustical external excitation, as well as by structural vibration on the boundaries.

From the indirect acoustical formulation, the following equation can be derived for the fluidum:

$$[-\omega^2 M^f - i\omega C^f + K^f]\{p\} = \rho\{\dot{q}\} + \omega^2\{l_f\} \tag{3}$$

with

M^f, C^f, K^f	matrices describing the pressure-volume acceleration relation in case of a rigid wall structure: these matrices do not reflect directly physical properties of the fluidum, but result from an indirect formulation of the acoustical problem.	
$\omega^2 \{l_f\} = \omega^2 \int_{s_b} \rho x_N dS$	the loading due to (normal) vibration x_N at the boundary s_b of the cavity	(4)

Rewriting and combining the two equations (1) and (3) results in the description of the vibro-acoustical coupled system.

$$\begin{bmatrix} K^s & -K^c \\ o & K^f \end{bmatrix} \begin{Bmatrix} x \\ p \end{Bmatrix} - i\omega \begin{bmatrix} C^s & o \\ o & C^f \end{bmatrix} \begin{Bmatrix} x \\ p \end{Bmatrix} - \omega^2 \begin{bmatrix} M^s & o \\ M^c & M^f \end{bmatrix} \begin{Bmatrix} x \\ p \end{Bmatrix} = \begin{Bmatrix} f \\ \rho\dot{q} \end{Bmatrix} \tag{5}$$

From (2) and (4) it can be seen intuitively that M^c and K^c are related to each other. Also according to reference [1], the elements of the matrices K^c and M^c can be expressed as follows (with n the normal to the surface; N_i, N_j finite element interpolation functions) :

$$K^c_{ij} = \int_{s_b} \underline{N}_i . \underline{n} N_j dS \tag{6}$$

$$M^c_{ji} = \int_{s_b} \rho N_i \underline{N}_j . \underline{n} dS \tag{7}$$

This indicates that both matrices are (in a transposed form) interrelated with a factor of ρ, the fluid density.

The set of equations (5) represents a second order model formulation for the vibro-acoustical behaviour and can be used as a basis for further deduction. However, it is clear that the set of equations is non-symmetrical. This is even more clear when rewriting equation (5) into a more compact matrix form :

$$\begin{bmatrix} A^s & -K^c \\ -\omega^2 M^c & A^f \end{bmatrix} \begin{Bmatrix} x \\ p \end{Bmatrix} = \begin{Bmatrix} f \\ \rho\dot{q} \end{Bmatrix} \tag{8}$$

with $A^s = K^s - i\omega C^s - \omega^2 M^s$ (9)

$A^f = K^f - i\omega C^f - \omega^2 M^f$ (10)

3. VIBRO-ACOUSTICAL RECIPROCITY

Reciprocity in purely structural vibration problems, as well as in purely acoustical pressure problems is well known. In the structural case, acceleration response and force are related, while in the acoustical case, volume acceleration and pressure are related.

For vibro-acoustical coupled problems, the vibro-acoustical reciprocity principle is valid. According to publications (e.g. [2],[3],[9]) this reciprocity is expressed as follows:

$$\frac{p_i}{f_j}\Big|_{\dot{q}_i=o} = \frac{-\ddot{x}_j}{\dot{q}_i}\Big|_{f_j=o} \tag{11}$$

In words, the ratio between the acoustical pressure response p_i at response location i within a cavity and structural force excitation f_j at a location j on the structure (without excitation by an acoustical source) equals the ratio between the acceleration response $\ddot{x}_j$ measured at the location and in the direction of the applied force j and acoustical excitation (expressed in volume acceleration) $\dot{q}_i$ at the pressure measurement location i (in absence of structural excitation).

This basic reciprocity principle is also reflected in the set of equations (8) that describe the coupled vibro-acoustical problem.

When only structural excitation is applied and no acoustical excitation ($!f;\dot{q}=o$), the following set of equations is valid:

$$\begin{aligned} A^s x - K^c p &= f \\ -\omega^2 M^c x + A^f p &= o \end{aligned} \tag{12}$$

Similarly, when only acoustical excitation is applied ($!\dot{q};f=o$):

$$\begin{aligned} A^s x - K^c p &= o \\ -\omega^2 M^c x + A^f p &= \rho\dot{q} \end{aligned} \tag{13}$$

By elimination and ordering follows:

$$\frac{p}{f}\Big|_{\dot{q}=o} = \left(A^s \frac{M^{c-1}}{\omega^2} A^f - K^c\right)^{-1} \tag{14}$$

$$\frac{\ddot{x}}{\dot{q}}\Big|_{f=o} = \left(\frac{M^c}{\rho} - A^f \frac{K^{c-1}}{\rho\omega^2} A^s\right)^{-1} \tag{15}$$

From equations (6) and (7), one can deduce that $M^c = \rho K^{c-1}$, which allows to write the following:

$$\frac{p}{f}\Big|_{\dot{q}=o} = \left(A^s \frac{K^{c\,t-1}}{\rho\omega^2} A^f - K^c\right)^{-1} \tag{16}$$

$$\frac{\ddot{x}}{\dot{q}}\Big|_{f=o} = \left(K^{c\,t} - A^f \frac{K^{c-1}}{\rho\omega^2} A^s\right)^{-1} \tag{17}$$

When the submatrices A^s, A^f, K^c and M^c are symmetrical the reciprocity relation (11) can be deduced from this set of equations.

The importance of equation (8) lies in the fact that vibro-acoustical reciprocity is valid, even if the describing set of equations is not symmetrical. However, symmetry of the submatrices is required, but this is a priori met under a linear assumption. The non-symmetry of (8) is a particular feature of coupled vibro-acoustical systems, and it differs both from the mechanical and acoustical subsystems, where reciprocity is expressed by the symmetric form of the governing equations as well. In other words, the intrinsic and more general feature of reciprocity of physical systems is not necessarily accompanied by symmetry in the mathematical description.

It is worth noting that the non-symmetrical formulation of the set of equations is due to the choice of variables $x, p, f, \dot{q}$ which is imperative to come to the second order formulation as described in equation (8). By using other sets of variables (e.g. $(x, p, f, \int q)$), the term ω^2 appears in A^f rather than in M^c in equation (8), rendering the equation symmetrical and enabling to use symmetrical (and more effective) numeric solvers for extracting the eigenvalues in FE calculations. However, this formulation is no longer a second order formulation and therefore it is not suitable to be used in standard experimental modal analysis (EMA) techniques. To the authors' knowledge no formulation has been put forward which is symmetric, corresponds to the presently used EMA formulation, and at the same time uses easily measurable acoustical parameters.

4. IMPLICATIONS FOR THEORETICAL VIBRO-ACOUSTICAL MODAL ANALYSIS

From the set of equations (5), it is clear that both the acoustical uncoupled problem and the vibrational uncoupled problem (K^c, $M^c = o$) can be described by a symmetrical set of second order equations. The same type of modal parameter estimation and modal decomposition algorithms as for vibrational problems can thus be used for acoustical problems.

For the vibrational uncoupled problem (measured) transfer characteristics x/f (displacement over force) are equivalent to the transfer characteristics $p/\dot{q}$ (acoustical pressure over volume acceleration of the acoustical sources) for the uncoupled acoustical problem.

For the coupled problem $K^c, M^c \neq o$ the set of second order equations (8) can be rewritten as :

$$\begin{bmatrix} A^s & -K^c \\ -\omega^2 \dfrac{M^c}{\rho} & \dfrac{A^f}{\rho} \end{bmatrix} \begin{Bmatrix} x \\ p \end{Bmatrix} = \begin{Bmatrix} f \\ \dot{q} \end{Bmatrix} \tag{18}$$

or

$$\begin{bmatrix} A^s & -K^c \\ -\omega^2 K^{c'} & A^{f^*} \end{bmatrix} \begin{Bmatrix} x \\ p \end{Bmatrix} = \begin{Bmatrix} f \\ \dot{q} \end{Bmatrix} \tag{19}$$

or in short notation :

$$[B] \begin{Bmatrix} x \\ p \end{Bmatrix} = \begin{Bmatrix} f \\ \dot{q} \end{Bmatrix} \tag{20}$$

The non-symmetry of the matrix $[B]$ implies that the right and the left eigenvalue problems give different solutions.

Conform to general modal analysis theory [6], it follows that a transfer function matrix $[H(p)]$ can be written as:

$$[H(p)] = [B(p)]^{-1} \tag{21}$$

with, based upon standard matrix calculation,

$$[B(p)]^{-1} = \frac{adj\,([B(p)])}{|\,B(p)\,|} \tag{22}$$

$adj\,([B(p)])$ is the adjoined matrix of $B(p)$

$$adj([B(p)]) = [\varepsilon_{ij}\,|\,B_{ij}\,|]' \tag{23}$$

with

$|\,B_{ij}\,|$ the determinant of $B(p)$ without row i and column j

$\varepsilon_{ij} = 1$ if $(i+j)$ is even, and

$\varepsilon_{ij} = -1$ if $(i+j)$ is odd

$|\,B(p)\,|$ the determinant of $B(p)$.

With λ_r the roots of the characteristic system equation $|\,B(p)\,| = 0$, (21) can be rewritten as :

$$[H(p)] = \frac{adj\,([B(p)])}{E \prod_{r=1}^{N} (p-\lambda_r)(p-\lambda_r^*)} \tag{24}$$

E is a constant.

By applying the theory of partial fraction expansion :

$$[H(p)] = \sum_{r=1}^{N} \frac{[A]_r}{(p-\lambda_r)} + \frac{[A]_r^*}{(p-\lambda_r^*)} \tag{25}$$

with

$\lambda_r,\ \lambda_r^*$	the complex conjugate pair of eigenvalues of the system matrix $B(p)$, or the roots of the characteristic equation
$[A]_r,\ [A]_r^*$	the complex conjugate residue matrices
N	the number of modes in the frequency band of interest.

In order to relate the residue matrices $[A]_r,\ [A]_r^*$ to the left and right eigenvectors of the system matrix $[B(p)]$ the following considerations can be made.

The residues equal :

$$[A]_r = ([H(p)]\ (p-\lambda_r))\ |_{p=\lambda_r} \tag{26}$$

or

$$[A]_r = \frac{adj\ ([B(\lambda_r)])}{\prod_{s=1, s\neq r}^{N} E \cdot (\lambda_r-\lambda_s)\ (\lambda_r-\lambda_s^*)\ (\lambda_r-\lambda_r^*)} \tag{27}$$

or

$$[A]_r = P_r \cdot adj\ ([B(\lambda_r)]) \tag{28}$$

with P_r a pole dependent constant

Equation (22) can be rewritten by right multiplication with $[B(p)]$ as :

$$adj\ |B(p)| \cdot B\ (p) = |B(p)|\ [I] \tag{29}$$

and by left multiplication with $[B(p)]$ as :

$$B(p) \cdot adj\ ([B(p)]) = |B(p)|\ [I] \tag{30}$$

Evaluating the equation (29) at the eigenvalues λ_r, gives, since λ_r is a root of the characteristic equation :

$$adj\ ([B(\lambda_r)]) \cdot [B(\lambda_r)] = 0 \tag{31}$$

This equation shows the proportionality between the adjoined matrix and the left eigenvector of the following eigenvalue problem :

$$\psi_l' \cdot [B(\lambda_r)] = 0 \tag{32}$$

From equation (30) it follows:

$$[B(\lambda_r)] \cdot adj\ ([B(\lambda_r)]) \quad = \quad 0 \tag{33}$$

Also the adjoined matrix is proportional to the right eigenvector:

$$[B(\lambda_r)] \cdot \psi_r \quad = \quad 0 \tag{34}$$

Considering any arbitrary row (i) of equation (31) or any arbitrary row (j) of equation (33) shows that each row (i) of the adjoined matrix is proportional to the left eigenvector ψ_l and that each column (j) of the adjoined matrix is proportional to the right eigenvector ψ_r, which in case of a non-symmetrical system are different from each other. This makes that the adjoined matrix can be written as :

$$adj \quad ([B(\lambda_r)]) \quad = \quad R_r \begin{bmatrix} (\psi_{1l}\psi_{1r}) & (\psi_{2l}\psi_{1r}) & (\psi_{3l}\psi_{1r}) & \cdots \\ (\psi_{1l}\psi_{2r}) & (\psi_{2l}\psi_{2r}) & (\psi_{3l}\psi_{2r}) & \cdots \\ (\psi_{1l}\psi_{3r}) & \cdots & \cdots & \cdots \\ \cdots & \cdots & \cdots & \cdots \end{bmatrix} \tag{35}$$

R_r is a constant.

For the special non-symmetry of the system equation (19) it can be proven that the right and the left eigenvectors show a special relation with respect to each other. Let the right eigenvectors be named $\begin{bmatrix} \psi_{sr} \\ \psi_{fr} \end{bmatrix}$, then the left eigenvectors $\begin{bmatrix} \psi_{sl} \\ \psi_{fl} \end{bmatrix}$ can be written as (subscript s is indicative for the structural response locations, subscript f for the acoustical response locations):

$$\begin{bmatrix} \psi_{sl} \\ \psi_{fl} \end{bmatrix}_{\lambda_r} \quad = \quad \begin{bmatrix} \psi_{sr} \\ \dfrac{1}{\lambda_r^2}\psi_{fr} \end{bmatrix}_{\lambda_r} \tag{36}$$

This can be proven (see also reference [7]) by substituting the values for the left eigenvectors (36) in the corresponding left eigenvalue problem formulation (32) and by transposing the matrix equation. Based upon the assumption of symmetry of both the structural and the acoustical submatrices A^s and A^{f^*}, and upon the assumption of symmetry of the coupling matrix K^c, this indeed yields the right eigenvalue problem with the corresponding right eigenvectors.

This leads to the following conclusions about the modal description of the coupled vibro-acoustical system, which are in correspondence with reference [5].

The transfer functions between structural displacement x_i or acoustical pressure response p_i at location i and structural force excitation f_j at location j can be written as a function of the right eigenvectors and eigenvalues of the system matrix, as follows, based upon equations (25), (28), (35), and (36):

$$\frac{x_i}{f_j} \quad = \quad \sum_{r=1}^{N} \frac{P_r\ \psi_{sri}\ \psi_{srj}}{(p-\lambda_r)} \quad + \quad \frac{(P_r\ \psi_{sri}\ \psi_{srj})^*}{(p-\lambda_r^*)} \tag{37}$$

$$\frac{p_i}{f_j} = \sum_{r=1}^{N} \frac{P_r \, \psi_{fri} \, \psi_{srj}}{(p - \lambda_r)} + \frac{(P_r \, \psi_{fri} \, \psi_{srj})^*}{(p - \lambda_r^*)} \tag{38}$$

The transfer functions between structural displacement x_i or acoustical pressure response p_i at location i and acoustical volume acceleration excitation $\dot{q}_j$ at location j can be written as follows:

$$\frac{x_i}{\dot{q}_j} = \sum_{r=1}^{N} \frac{P_r \, \psi_{sri} \, \psi_{frj}}{\lambda_r^2 (p - \lambda_r)} + \frac{(P_r \, \psi_{sri} \, \psi_{frj})^*}{\lambda_r^2 (p - \lambda_r^*)} \tag{39}$$

$$\frac{p_i}{\dot{q}_j} = \sum_{r=1}^{N} \frac{P_r \, \psi_{fri} \, \psi_{frj}}{\lambda_r^2 (p - \lambda_r)} + \frac{(P_r \, \psi_{fri} \, \psi_{frj})^*}{\lambda_r^2 (p - \lambda_r^*)} \tag{40}$$

The right eigenvectors of the coupled problem represent (but for a global scale factor) the vibro-acoustical modes; the left eigenvectors represent (but for a scale factor per mode) the participation factors. Due to the special relation between left and right eigenvectors, the participation factors for acoustical excitation and structural excitation are different with a scale factor that equals the eigenvalue squared (and thus different from mode to mode).

5. IMPLICATIONS FOR EXPERIMENTAL VIBRO-ACOUSTICAL MODAL ANALYSIS

Most of the multiple input / multiple output modal parameter estimation algorithms do not require symmetry. The non-symmetry of the basic set of equations (19) and hence of the modal description (37) - (40) does not pose as such any problems for those parameter estimation techniques, in order to obtain valid modal frequencies, damping factors, and mode shapes. The non-symmetry of the model is absorbed by the participation factors.

Structural excitation can be substituted by acoustical excitation (see equations (37) to (40)). The modal models (mode shapes, frequencies and damping factors) derived from either acoustical excitation FRFs or structural excitation FRFs are compatible, taking into consideration the normal excitation controlability restrictions. However, the participation factors, obtained with acoustical excitation, differ by a scale factor per mode, as related to structural excitation, this due to the special non-symmetry of the set of equations.

This has its consequences in expanding the system matrix from one type of excitation to another type of excitation. For purely structural applications, the expansion is symmetrical, based on the structural reciprocity principle. In vibro-acoustical systems, the expansion must be done according to the vibro-acoustical reciprocity principle, which means that the expansion from one excitation type to the other cannot be done in a symmetrical way. This is reflected in the scale factors that must be applied, in order to go from the structural formulation (37)-(38) to the acoustical formulation (39)-(40). The scaling factors are the squared eigenvalue for each corresponding mode.

For practical applications, acoustical excitation is preferred over structural excitation for different reasons: the measurements are of better quality, the acoustics of the cavity which is the goal function to be studied is excited in a direct way, the measurements are more efficient. There is however a very important practical aspect: how to determine the quantity $\dot{q}$ (volume acceleration) of the acoustical source. Although commercially available systems do not yet exist, various techniques have been suggested [8] and are in use with success since quite some time. The methods used for the application part in this paper will be discussed in 6.2.

6. APPLICATION : MEASUREMENTS AND ANALYSIS ON A VIBRO-ACOUSTICAL MODEL

6.1 Model description

The model used for the experiments is an irregular PVC box (with some resemblance to a car body) of maximum dimensions 0.84x0.4x0.4 m, plate thickness 0.01 m. By using a large number of screws in order to prevent clearance, the box can either be closed with a PVC bottom plate (for the uncoupled acoustical case) or with a flexible steel plate of 0.001 m thickness (for the vibro-acoustical coupled case). A third possible version of the setup can be obtained by removing the three top plates, thus bringing about nearly uncoupled conditions for the flexible bottom plate (uncoupled structural case).

The acoustical excitation is ensured by a loudspeaker provided with a closed back cavity, built in in one of the upper corners of the model box. It can be taken out and replaced by a rigid PVC plate during the structural excitation measurements, in order to close the cavity with uniform impedance everywhere. For the structural excitation two shakers are used, which are decoupled during the acoustical excitation experiments, in order again to avoid any uncontrolled impedance constraints. The references for the structural excitation are measured by force transducers, the structural responses are measured by means of a set of roving accelerometers. The reference for the acoustical excitation, volume acceleration of the acoustical source, is derived from the input voltage to the loudspeaker (to be discussed below in more details). The acoustical responses are measured by means of a roving array of 5 miniature electret microphones. The total number of structural responses was 212, the number of acoustical responses was 151 (including driving point measurements). Figure 1 shows the picture of the experimental setup.

6.2 Acoustical source calibration

The correct calibration of the acoustical source is essential if one aims at proving vibro-acoustical reciprocity in quantitative terms. The acoustical source is calibrated by laser velocity measurements at 31 points on the loudspeaker surface in the form of FRFs referenced to the input voltage, and this under anechoic conditions in a frequency range 20 to 1000 Hz. The volume acceleration vs. input voltage calibration function is then calculated as the average velocity over all points, multiplied by the active surface of the diaphragm of the loudspeaker and $j\omega$. Figure 2 shows the obtained calibration curve used throughout the measurement series. In order to establish whether or not the loudspeaker's output is unacceptably influenced by the loading impedance of the cavity during the actual measurements, the pressure in the back cavity of the loudspeaker

referenced to the input voltage is measured as well, both during calibration, and during the actual measurement runs. Figure 3 shows the superposition of the backcavity pressure/voltage FRF during calibration (under free field conditions (solid line)) and during measurement (loudspeaker in enclosed cavity (dashed line)). Clearly the effects of the acoustical resonances of the cavity can be seen, but are nevertheless negligable. This implies that the input voltage of the loudspeaker can be considered as a correct reference signal for the measurements.

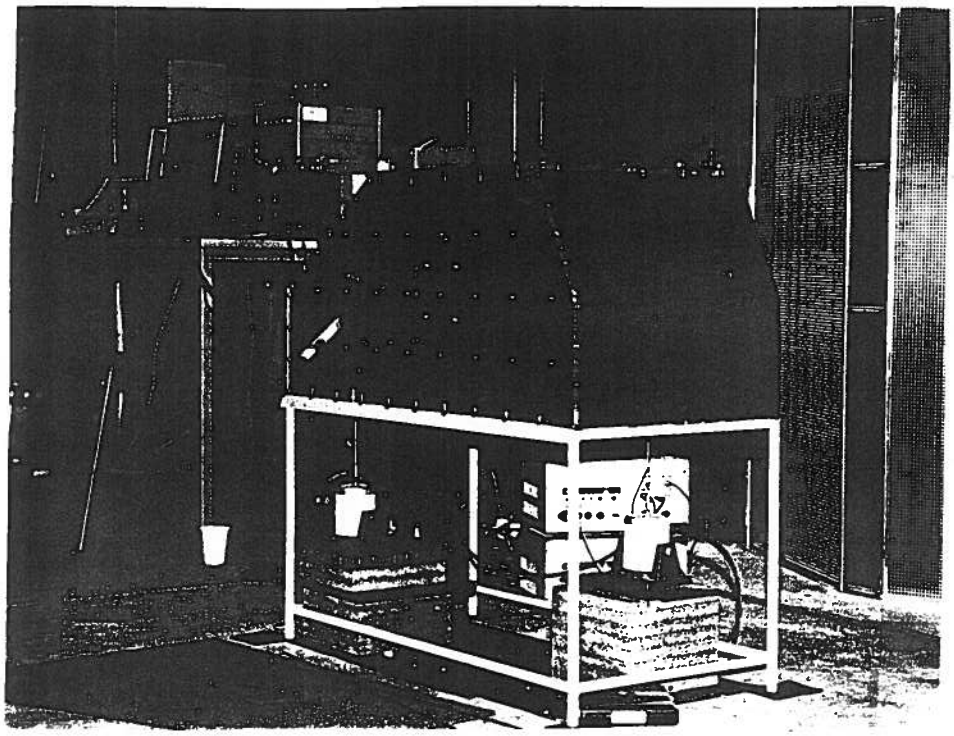

Figure 1 Experimental setup

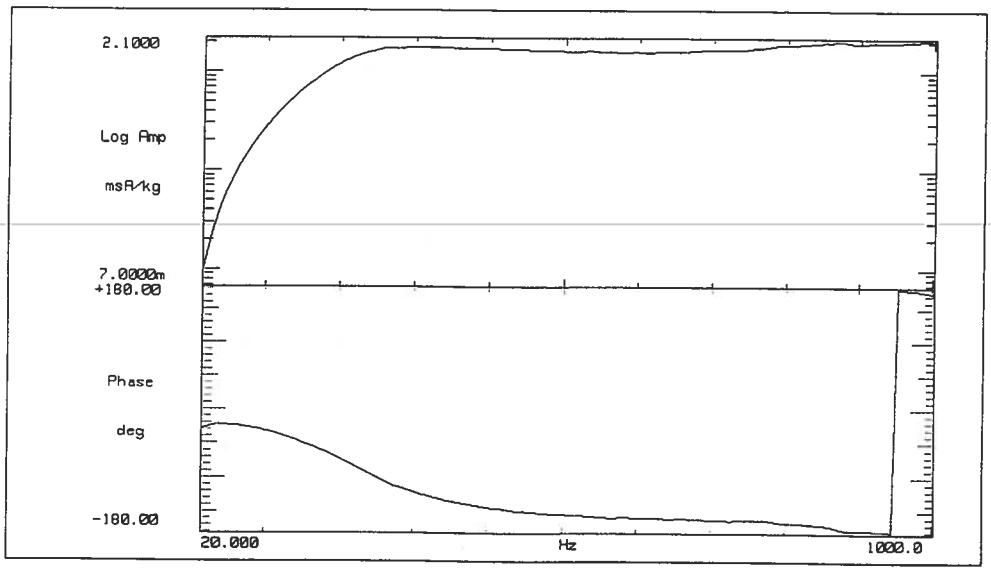

Figure 2 Calibration curve : volume acceleration/voltage FRF

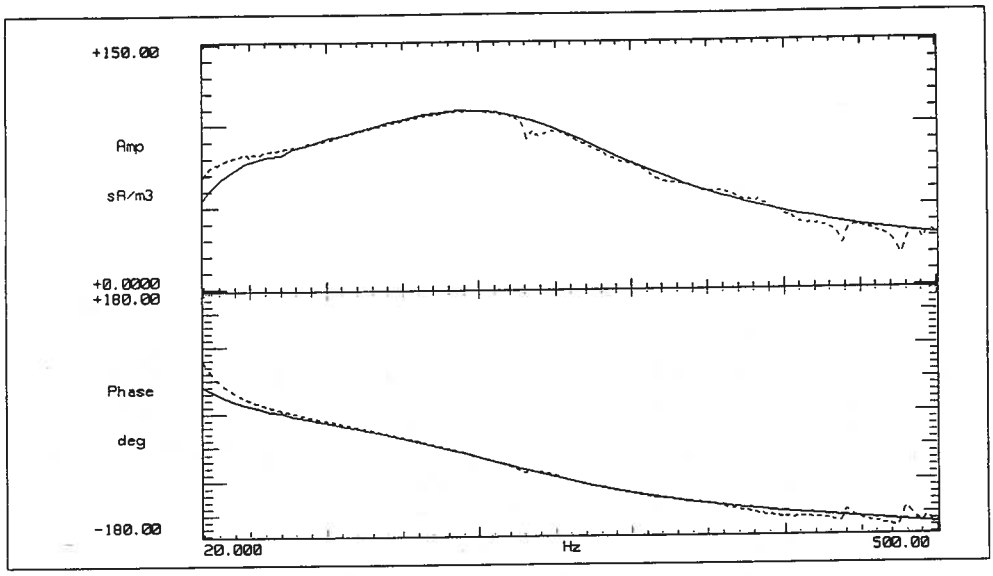

Figure 3 Backcavity pressure/voltage FRF in loudspeaker in free field and in enclosed cavity field

6.3 Measurements

In order to establish the effects of the vibro-acoustical coupling on the modal characteristics of the various systems investigated, three series of measurements are performed : one to reveal the characteristics of the flexible bottom plate of the box without cavity (uncoupled structural subsystem - (dual input) structural excitation, structural responses), one to determine the modal model of the cavity enclosed with rigid walls (uncoupled acoustical subsystem - (single input) acoustical excitation, acoustical responses), and eventually, measurements on the coupled vibro-acoustical system (both structural and acoustical excitation - both structural and acoustical responses). In the course of the measurements series only auto- and crosspowers were measured and stored. The calculation of the FRFs and the modal analysis were performed subsequentially.

Figure 4 gives the summed structural/structural FRFs for both the uncoupled structural case and the coupled case, between 210 Hz and 260 Hz (232 Hz is the first acoustical cavity mode). Figure 5 gives the summed acoustical/acoustical FRFs for both the uncoupled acoustical case and the coupled case. It is clear from figure 5 that the acoustical response in the cavity is remarkably affected by the coupling. A new resonance frequency emerges, while the original (uncoupled) resonance frequency essentially remains unchanged. The structural response is less sensitive, even though a thorough analysis shows the existence of a new peak in the data in the coupled case and a slight shift of the original resonance frequencies can also be observed.

Some global frequency shifts have occurred between coupled and uncoupled cases, which can be attributed to temperature shifts (in spite of all effort to keep measurement time as low as possible, the measurements had to be performed over several day's time) and to slightly varying boundary conditions in between the different measurement setups.

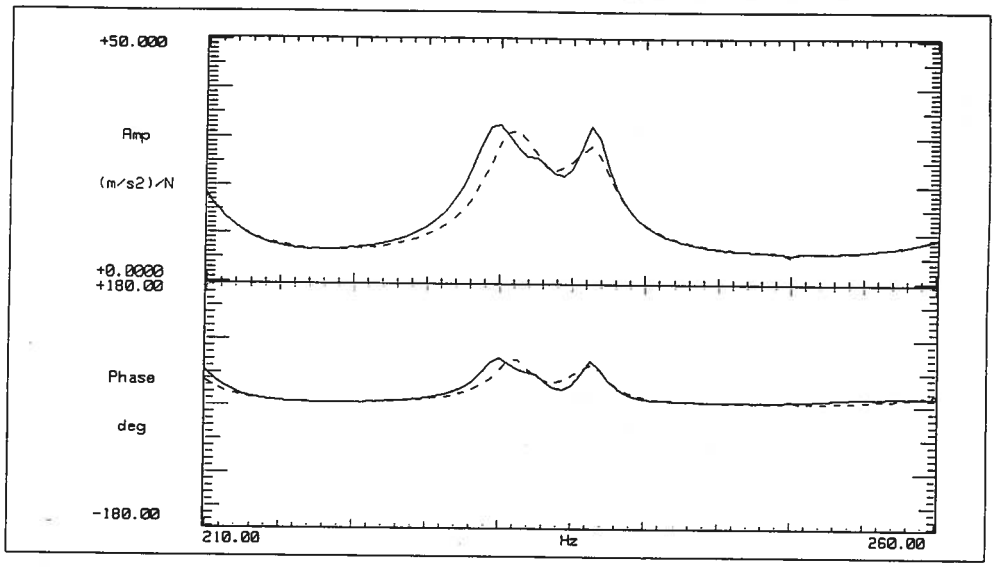

Figure 4 Summed structural/structural FRFs (coupled (solid) vs. uncoupled case (dash))

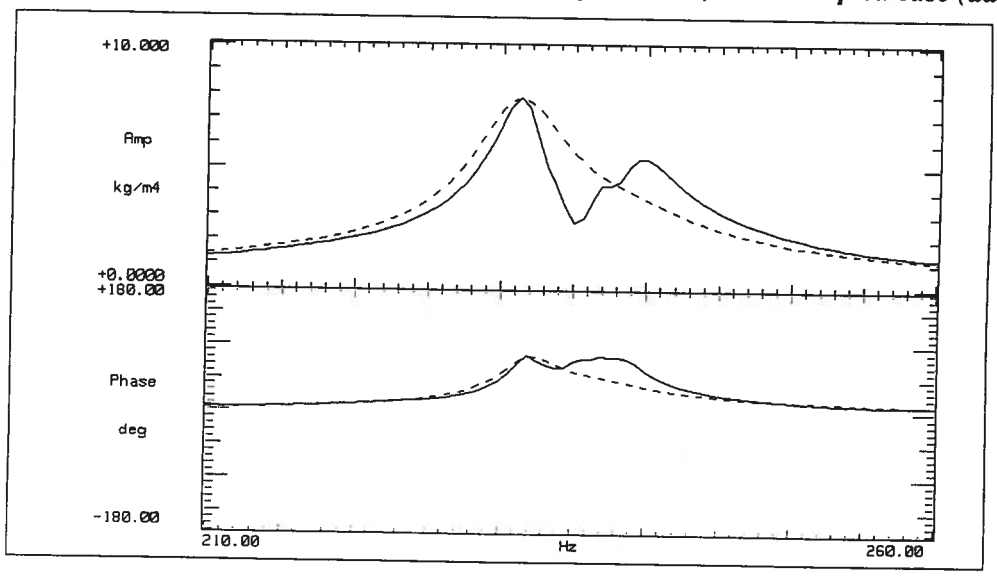

Figure 5 Summed acoustical/acoustical FRFs (coupled (solid) vs. uncoupled case (dash))

6.4 Vibro-acoustical reciprocity

Due to the absolute calibration of the acoustical source used in the experiment, the vibro-acoustical reciprocity can be really verified. Figure 6 shows the superposition of the FRFs of the acoustical pressure response at the loudspeakers location (with the loudspeaker taken away from the measurement set up and substituted by a rigid plate) with respect to structural excitation at one position, with the acceleration response at this shaker position with respect to acoustical excitation of the loudspeaker (with the shakers disconnected from the bottom plate). Figure 7 shows the same relationship for the second shaker position. Despite the rather bad quality (caused by low signal to noise ratio, due to the not sufficiently high level of excitation) the correspondence between the pairs of FRFs is rather convincing. It shows that the vibro-acoustical reciprocity is a valid assumption for this experimental system.

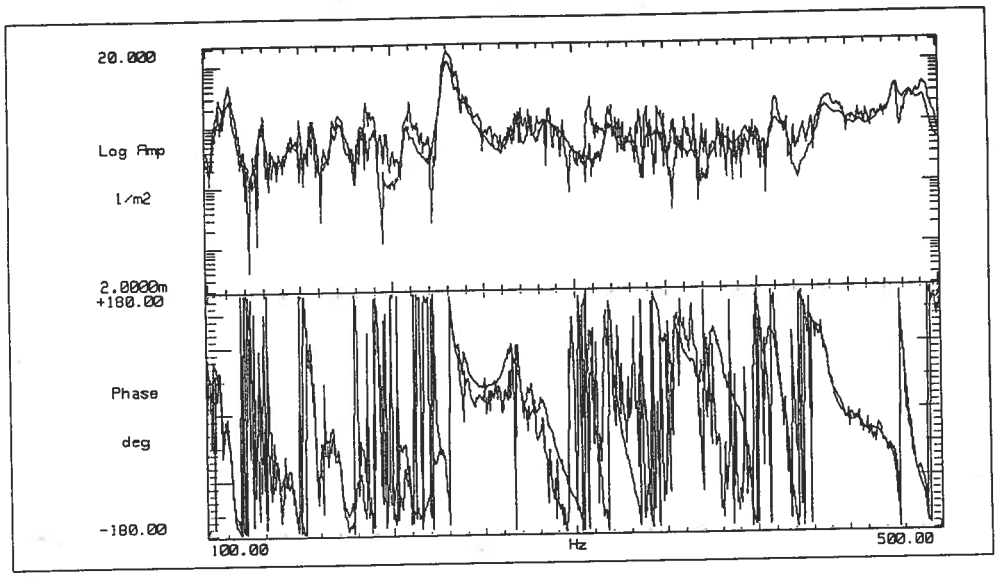

Figure 6 Vibro-acoustical reciprocity at shaker location 1

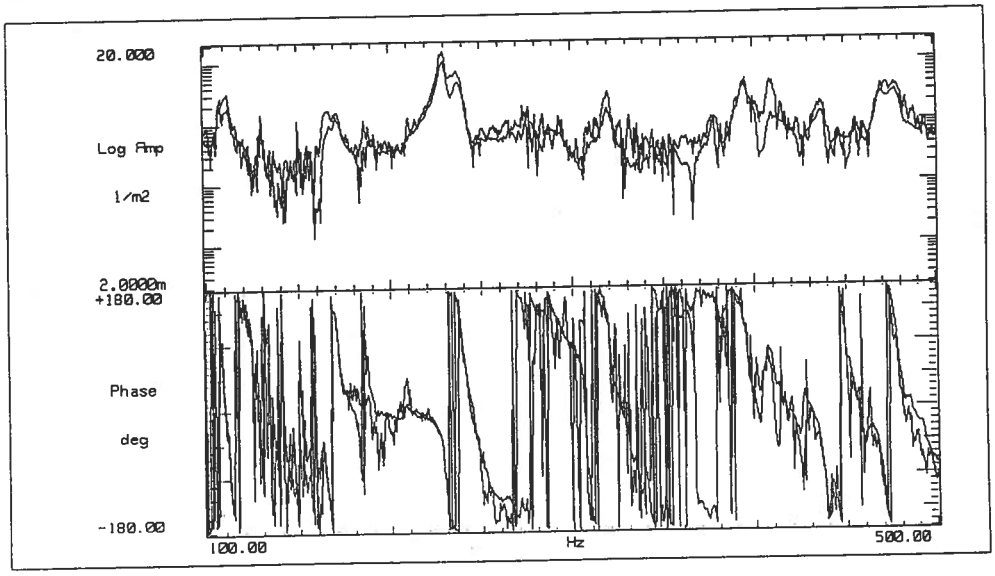

Figure 7 Vibro-acoustical reciprocity at shaker location 2

6.5 Modal analysis results

Least squares complex exponential and least squares frequency domain curve fitting procedures were used for curve fitting all available data. This resulted in the following natural frequencies, and damping factors for the different cases considered:

uncoupled acoustical	uncoupled structural	coupled structural excitation	coupled acoustical excitation
	230.8 Hz / 0.8%	230.0 Hz / 0.7%	231.8 Hz / 0.7%
230.9 Hz / 1.4%		232.6 Hz / 0.6%	233.6 Hz / 0.5%
		236.3 Hz / 0.5%	237.2 Hz / 0.5%
	236.4 Hz / 0.6%	238.1 Hz / 0.9%	238.4 Hz / 1.0%

Figures 8 to 11 show the corresponding mode shapes. The pressure variation in the acoustical cavity is represented by a "displacement" perpendicular to the planes that were measured in the cavity. Clearly both the coupled structural modes and the acoustical modes correspond very well between the structural excitation case and the acoustical excitation case. The coupled acoustical modes are very similar to the non-coupled acoustical mode shape; the coupled structural modes are very clearly related to the original uncoupled structural mode shapes.

6.6 Reciprocal extrapolation

As mentioned above, the extrapolation from one type of excitation to the other type of excitation requires a vibro-acoustical reciprocal extrapolation, which is not symmetrical. As an example the synthesis of acoustical responses due to structural excitation at some point requires special scaling of the modal model, obtained by acoustical excitation. If this scaling is not taken into account, the obtained synthesis will not be correct. The synthesis of the FRF between a pressure at point k and a force at point m is calculated as a combination of FRFs obtained via acoustical excitation in the following way. Assume t the location of acoustical excitation, and assume a driving point acoustical FRF has been measured, then the following can be written :

$$\frac{p_k}{f_m} = \frac{p_k}{\dot{q}_t}\frac{\dot{q}_t}{p_t}\frac{p_t}{f_m} \tag{41}$$

The first two FRFs in the multiplication are known directly, synthesised from the acoustical excitation modal model. The third FRF (a structural excitation FRF, which can be expressed by (38)) must be deduced from the reciprocal acoustical excitation FRF (as expressed by (39)). Combining these two equations indeed introduces for each mode shape in the synthesis a factor λ_r^2.

As an example the synthesis of an acoustical response due to structural excitation is done, derived from an acoustical excitation modal model. Figure 12 shows the superposition of the FRFs synthesised with and without appropriately scaling the acoustical excitation modal model, before expanding it to the structural excitation case. Clearly large scaling deviations exist between the two synthesised FRF. Figure 13 then shows the synthesis of the structural excitation FRF with the appropriately scaled acoustical excitation modal model, together with a synthesised FRF from the structural excitation modal model. The differences are mainly due to the shift in natural frequencies that were observed during the tests. It is clear that the magnitude of the FRFs are corresponding quite well.

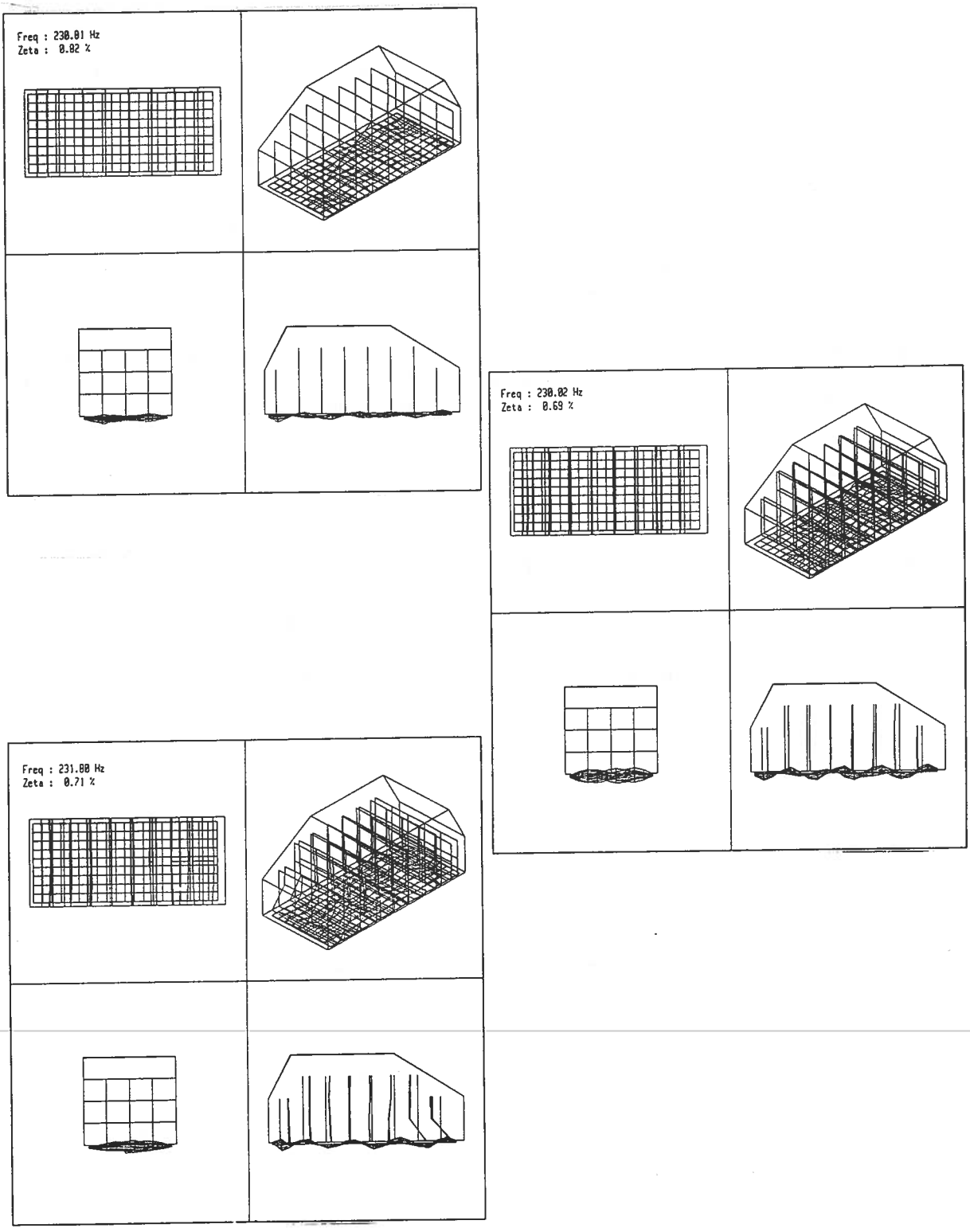

Figure 8 Modal deformations : upper figure : uncoupled structural case; middle figure : coupled case structural excitation; lower figure : coupled case acoustical excitation

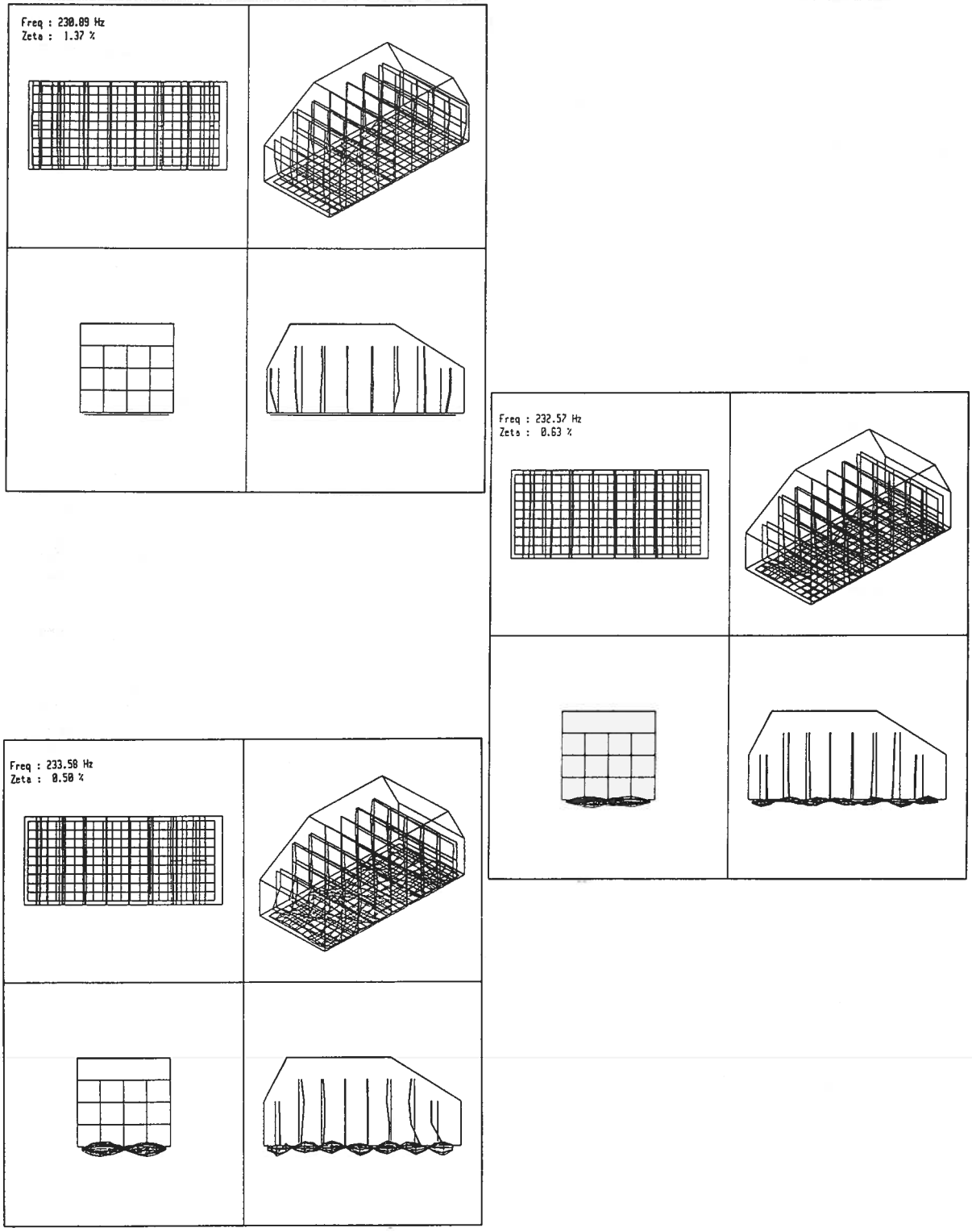

Figure 9 Modal deformations : upper figure : uncoupled acoustical case; middle figure : coupled case structural excitation; lower figure : coupled case acoustical excitation

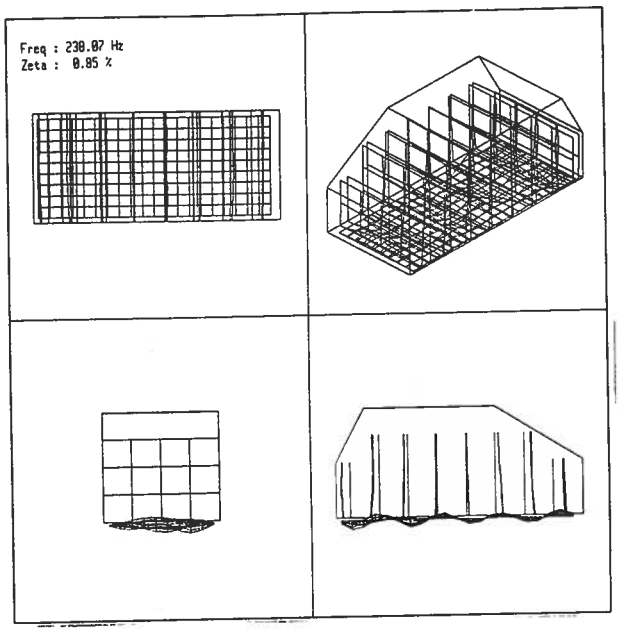

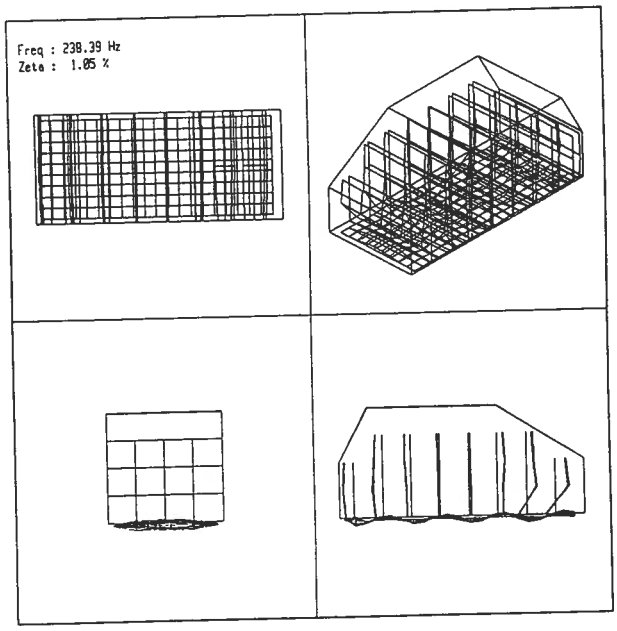

Figure 10 Modal deformations : upper figure : coupled case structural excitation; lower figure : coupled case acoustical excitation

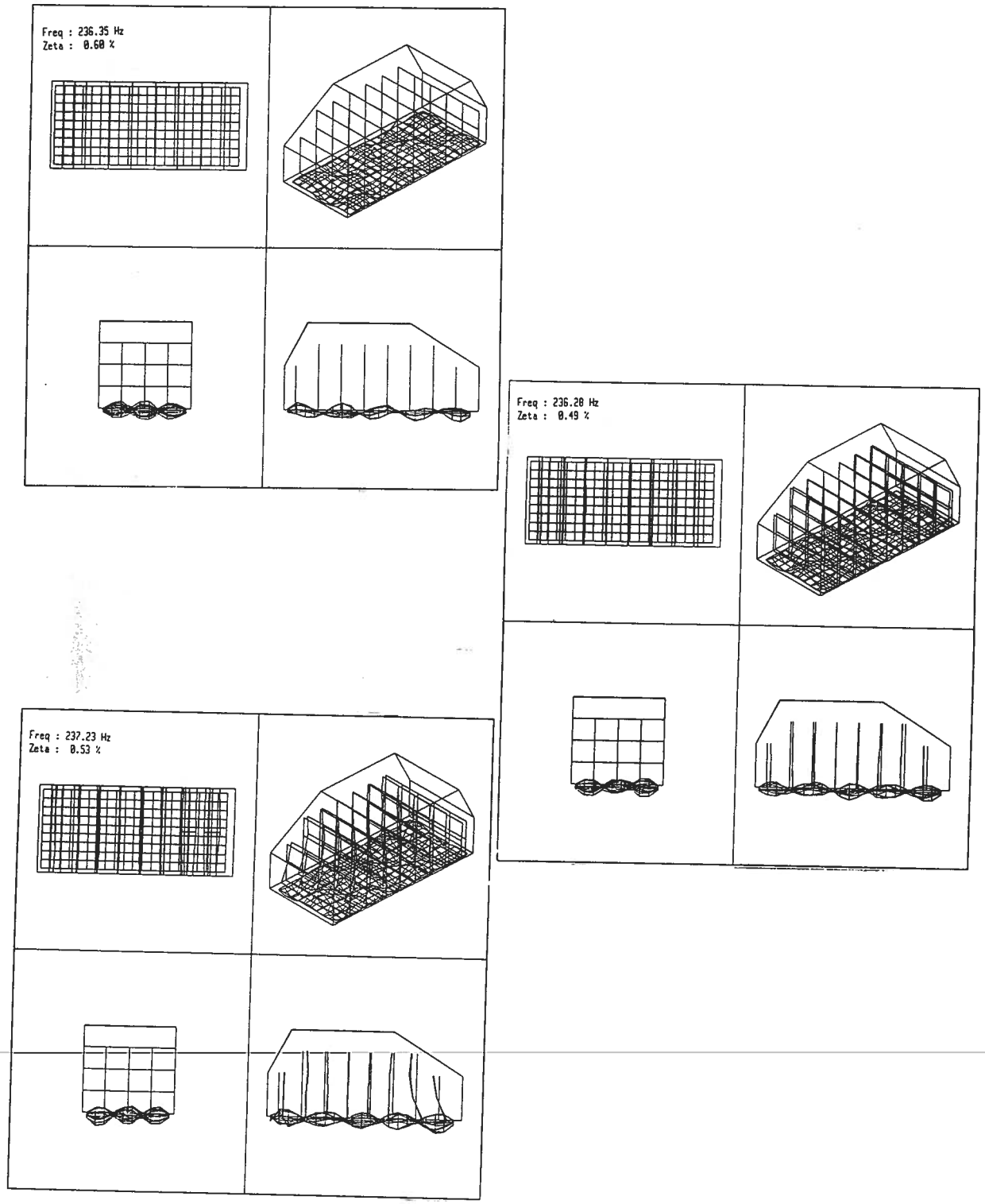

Figure 11 Modal deformations : upper figure : uncoupled structural case; middle figure : coupled case structural excitation; lower figure : coupled case acoustical excitation

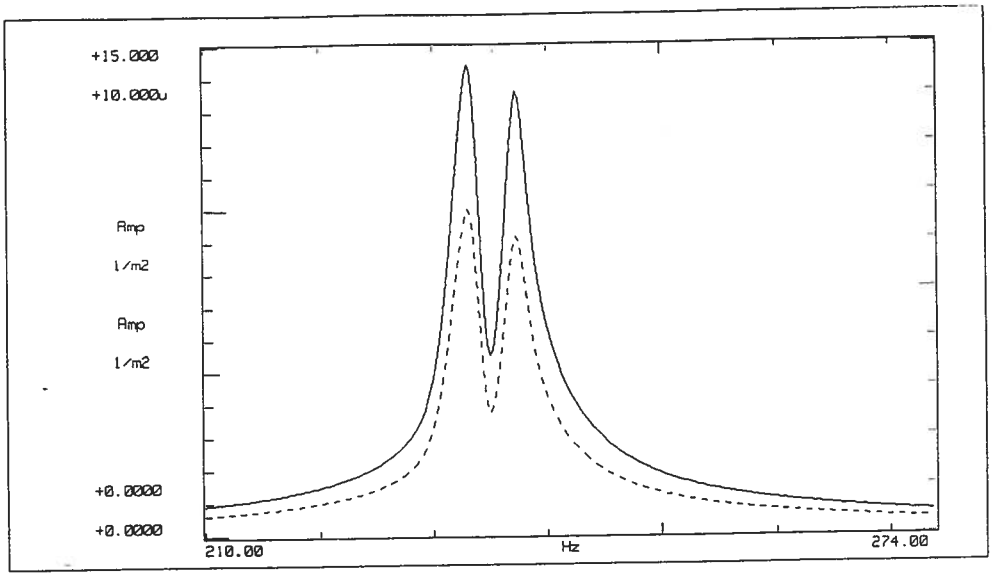

Figure 12 Synthesis of acoustical response/structural excitation FRF based on a scaled (solid line) and a non-scaled (dash line) acoustical excitation modal model (note the difference in ordinate scales)

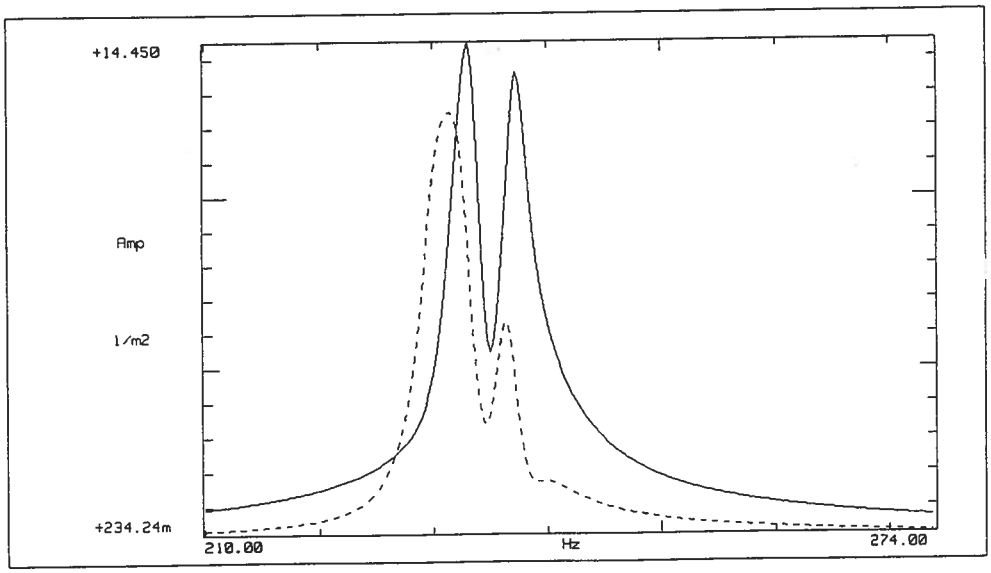

Figure 13 Synthesis of acoustical response/structural excitation FRF based on a scaled acoustical excitation modal model (solid line) and on a structural excitation modal model (dash line)

7. CONCLUSIONS

Within this paper a framework of reference has been put down for performing vibro-acoustical modal analysis. Starting from a theoretical finite element formulation of the vibro-acoustical problem, it is shown which second order model formulation is appropriate and consistent for experimental vibro-acoustical modal analysis. It is explained which physical parameters must be measured, both in case of structural excitation and in case of acoustical excitation. Also it is shown

that the general vibro-acoustical reciprocity does not imply model symmetry. On the contrary, the equations of motion are characterised by a special non-symmetry. The consequence of this is that special modal scaling, equal to the eigenvalues squared, must be applied in the modal models to go from acoustical excitation to structural excitation, and vice versa.

The theory is proven by performing extensive structural and acoustical tests, both using structural and acoustical excitation, on a vibro-acoustical laboratory model. Care is taken to calibrate the acoustical source strength. By this vibro-acoustical reciprocity can be verified and proven experimentally. Consistent modal models are derived from the FRFs obtained with structural and acoustical excitation. The need for scaling the modal models when going from one type of excitation to another is demonstrated.

8. ACKNOWLEDGMENTS

We want to thank Jan Dessein for his involvement in the measurements, which were carried out with a lot of tedious patience.

REFERENCES

[1] P. Göransson, **Acoustic Finite Elements**, *Proc. Advanced Techniques in Applied and Numerical Acoustics, International Seminar on Applied Acoustics, 31/08-02/09,1992, ed. P. Sas, Leuven (B).*

[2] F.J. Fahy, **The reciprocity Principle and Application in Vibro-acoustics**, *Proc. 2nd International Congress on Recent Developments in Air- and Structure-Borne Sound and Vibration, 1992.*

[3] P.J.G. van der Linden, J.K. Fun, **Using Mechanical-Acoustic Reciprocity for Diagnosis of Structure-Borne Sound in Vehicles**, *Proc. 1993 Noise and Vibration Conference, SAE P-264, 1993.*

[4] F. Augusztinovicz, **Acoustic Modal Analysis**, *Proc. Advanced Techniques in Applied and Numerical Acoustics, International Seminar on Applied Acoustics, 31/08-02/09,1992, ed. P. Sas, Leuven (B).*

[5] Q. Zhang, **Application de l' Analyse Modale à la Résolution des Problèmes Acoustiques Automobiles en Basse Fréquence**, *Journal SIA 380, pp 44-50, 1993.*

[6] W. Heylen, P.Sas, S. Lammens, **Modal Analysis Theory and Testing**, *18th International Seminar on Modal Analysis, Leuven, 1993.*

[7] Z.D. Ma, I. Hagiwara, **Sensitivity Analysis Methods for Coupled Acoustic-Structural Systems Part I : Modal Sensitivities**, *AIAA Journal, vol.29, nr. 11, 1991.*

[8] R. Singh, M. Schary, **Acoustic Impedance Measurement using Sine Sweep Excitation and known Volume Velocity Technique**, *J. Acoust. Soc. Amer. 64 (4) 995-1005, 1978.*

[9] J.W. Verheij, **Multi-path Sound Transfer from Resiliently Mounted Shipboard Machinery**, *PhD thesis, 1982, Delft*

[10] J.W. Verheij, **Experimental Procedures for Quantifying Sound Paths to the Interior of Road Vehicles**, *2nd Int. Conf. Vehicle Comfort, Oct 1992, ATA, Bologna*